

# *Chapter 1*

## *Introduction*

### **1.1 Overview**

Studying fast neutron-induced reactions at higher incident energies is interesting in fundamental and applied physics. The neutron induced reactions can describe reaction mechanisms and examine nuclear structure by restricting nuclear models in fundamental nuclear physics. Accurate nuclear data are needed for many practical applications, including nuclear energy, safety and security, safeguards, nuclear medicine, and planetary and space exploration. These applications rely on nuclear phenomena such as reaction cross section, decay, and structure data. In general, the cross sections are probabilistic values that represent the probabilities of specific reactions taking place given an incoming particle, a target nucleus, and the energy of the incident particle. The total production cross sections of the residual nucleus are generally obtained for ground state reaction products, although isomeric state production cross sections also explore our understanding of the level and decay structure of the residual nucleus [1].

Neutron activation analysis is a particularly effective approach because neutrons may penetrate deep into materials, providing information on the bulk rather than just the surface. A schematic diagram of the neutron activation analysis process is shown in Fig. 1.1. Application of the activation technique is particularly fruitful if the cross sections are 1 (*mb*) or more, the radioactive product has a half-life of several minutes to several days and its decay is accompanied by the emission of a  $\gamma$ -ray in the range from 100 keV to several MeV and an intensity of 10% or more. In such cases, the overall irradiation time, the total counting time, and the sample transfer time between irradiation and activity determination are very favourable, allowing relatively large scale measurement programs in a short time. Furthermore, the easy to use, highly selective, and well established high-purity germanium (HPGe) spectrometry can be used to determine the activity of the reaction products [2].

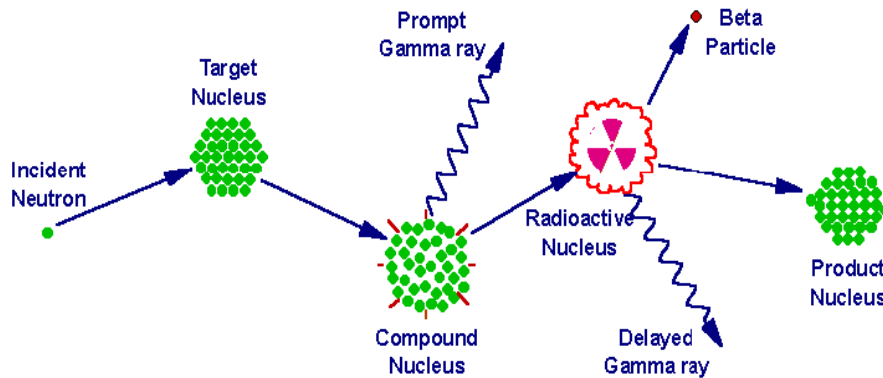


**Fig. 1.1** Schematic representation of Neutron Activation Analysis steps and illustration of the neutron induced reaction process.

Nuclear reactions are responsible for nucleosynthesis, or the production of elements throughout the Universe. The  $^2\text{H}$ ,  $^3\text{He}$ , and particles are the most common products of Big Bang nucleosynthesis. The development of early stars, which create elements up to Fe, follows this initial nucleosynthesis. Different mechanisms, like neutron capture, neutron induced reactions, explosive events in supernovae, and the rapid-neutron process in neutron star mergers, are used to create heavier elements. The neutron energy range between the 1 keV and 1 MeV is essential in astrophysics because it corresponds to the temperature regimes of the important areas for synthesizing all nuclei between iron and actinides.

Apart from the astronomical purpose, there is continued interest in neutron cross sections for practical applications, such as the neutron balance in modern reactors aiming for high burn-up rates and concepts dealing with radioactive waste transmutation. Determining  $(n, xn)$  reaction cross sections are essential for developing fast reactors since the neutron balance in the reactor core is affected by the neutron multiplication caused by such reactions. At moderately high temperatures, the  $(n, 2n)$  channel may dominate the  $(n, \gamma)$  reaction channel. This might be important in the nucleosynthesis of neutron rich isotopes and in the r-process nucleosynthesis. Therefore, testing the assumption that multiparticle emission is negligible at astrophysics relevant energy is necessary. For this reason, measurements of the cross section of the  $(n, 2n)$  reaction channel are important [3-4].

One of the most critical issues to resolve for public acceptability of nuclear fission energy generation is developing and controlling long-term radioactive danger. ADSs (Accelerator Driven Sub-Critical Systems) for nuclear waste transmutation offer a viable solution to this

challenge. A schematic diagram of the Accelerator Driven Sub-critical System (ADSs) is shown in Fig. 1.2. The system consisting of a sub-critical reactor and a spallation neutron source generated by a high-power accelerator with a heavy metal target, is fundamentally safe. This will be assured by online monitoring of the sub-criticality level that is both reliable and accurate. However, several obstacles must be overcome before the initial notion of ADSs can be achieved and its viability established. This is significant in the context of reactor physics and neutronics, where nuclear data uncertainties play a substantial role in determining many-core and fuel cycle parameters. Nuclear research reactors are crucial to the advancement of nuclear science and technology. They're utilized in fundamental research, radioisotope manufacturing, neutron scattering, radiography and material characterization and testing, among other applications [5-6].

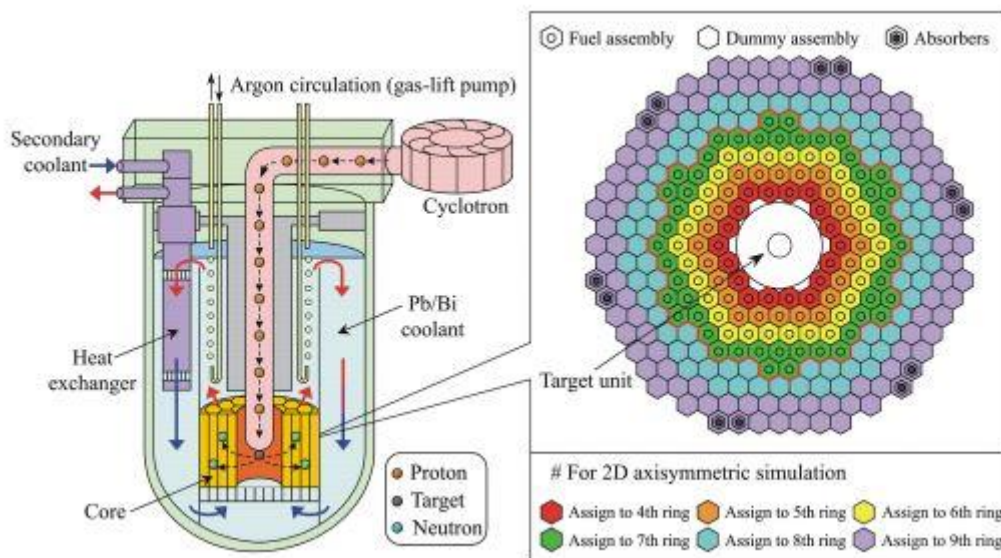


**Fig. 1.2** A schematic diagram of the Accelerator Driven Sub-Critical System (ADSs).

Since the early 1980s, several large and excellent measurement campaigns were conducted around 14 MeV to facilitate the knowledge of cross sections relevant to the fusion community. For higher energies, the interest in the range above 14 MeV and up to several GeV is a consequence of the study of accelerator-driven systems (since early 1990) and, more recently, of the design of the IFMIF materials irradiation facility for the study of radiation damage in fusion reactors (maximum energy 55 MeV). Even for such systems, the primary energy range of relevance in large part of the facility is below 20 MeV. The outcomes of the experiments may be used to investigate different statistical model codes and confine the parameter sets they used. Such research is also expected to shed light on the reaction

mechanisms in various energy regions. The information will be used to construct the International Fusion Material Irradiation Facility (IFMIF), which will test materials for fusion power plant technologies. Despite substantial improvements in the quality of nuclear data, such as neutron interaction cross sections, little information on nuclear data uncertainties and much less on nuclear data covariance are available. In nuclear applications, covariance data is necessary to examine design parameter uncertainties accurately [7].

The available database above 14 MeV is minimal, reflecting the lack of need for such data from traditional fission and fusion reactor development. Around 14 MeV, many measurements were performed because of the widespread use of neutron generators, but often these data show discrepancies and large scatter. Studies of cross sections and isomeric cross section ratio of neutron threshold reactions are of considerable significance for testing nuclear models and practical applications. The improved experimental data on neutron induced charged particle ( $n, p$ ) and ( $n, \alpha$ ) reactions on structural materials are essential and critical for defining processes like brittlement, nuclear heating, induced radioactivity, nuclear transmutation rates, and damage caused by hydrogen and helium generation in structural materials [8].

The elements V, Cr, Ti, and Cu based alloys have excellent properties that make them an essential structural material for reactor technology. In the fusion reactor, vanadium is considered the reactor structural material for the first wall/blanket applications due to the low activation properties of the vanadium alloys. Similarly, copper as a first wall material has been considered in reactor designs with high thermal loads on the first wall. It requires a shield of high electrically conductive material surrounding the plasma to help stabilize its location. Furthermore, because of their remarkable characteristics, Titanium and chromium alloys are desirable structural materials for fusion reactors. The activation data on titanium and chromium is important for practical applications in fusion reactor technology e.g., estimation of activity level, hydrogen and helium gas production, nuclear heating, and radiation damage since chromium is an important constituent of structural steel.

The elements  $^{78}\text{Se}$  and  $^{80}\text{Se}$  are also used as targets to produce  $^{77}\text{Br}$  and  $^{80\text{m}}\text{Br}$ , which are therapeutic radioisotopes. The ( $n, p$ ) reaction produces arsenic isotopes, which are poisonous to humans and other living creatures. Cancer and other serious health problems occur due to the arsenic element. The ( $n, 2n$ ) reaction cross sections of the  $^{121}\text{Sb}$ ,  $^{123}\text{Sb}$ , and  $^{103}\text{Rh}$  isotopes are essential for neutron multiplication calculations. Some of the antimony isotopes in nuclear fission have been identified as nuclides of the fission product. Therefore, fast neutron induced

reaction cross section measurements with better accuracy for antimony are essential for improving nuclear data. Threshold reactions, including  $(n, n')$  and  $(n, 2n)$  have been used extensively for determining the differential flux ( $dQ/dE$ ) from neutron sources by foil activation techniques. The cross sections of  $(n, xn)$  reactions are necessary for activation detectors which are used to probe energy components of neutron fluence. An example of such a detector is rhodium, which is monoisotopic. Thus, it is essential to study the higher energy neutron induced reaction cross section for Rh, Sb, V, Cr, Ti, Cu, and Se elements from an application point of view.

## 1.2 Nuclear Database

The nuclear data community maintains many databases for the use of its members as well as for the application communities. The suggested values for the evaluated data libraries are based on an expert review. There are also unevaluated libraries and databases where experimental data and computations are assembled and available for usage within and beyond the community. There are different data libraries which are mentioned below:

### 1.2.1 Experimental Nuclear Reaction Data (EXFOR)

The most extensive database of data on experimental nuclear reactions is now the EXFOR library. The GUI of the EXFOR database is shown in Fig. 1.3. The EXFOR began as a standard format for exchanging nuclear measurement results between multiple data centres. It includes nuclear reaction cross sections and other values produced by a neutron, charged particle, and photon beams. For every light charged particle ( $A \leq 12$ ) and low and moderate energy ( $\leq 1$  GeV) neutron induced reaction data, the compilation is currently required. Additionally, data on heavy ions ( $A \geq 13$ ) and photon induced reactions are gathered voluntarily. The first important phase in the data collection process is to search the literature for papers that describe experimental data for the EXFOR compilation. There are a large collection of experimental nuclear reaction data in the EXFOR (EXchange FORmat) library. The EXFOR database contains data of 24704 entries from experimental works. The EXFOR (EXchange FORmat) database includes cross section reaction data (50.9 %), partial differential data with respect to angle (19.4 %), differential data concerning angle (18.9 %), resonance parameters (8.58 %), partial cross section data (8.49), fission product yields (5.91 %), and other

topics *etc.* Since the discovery of the neutron, neutron reactions have been systematically compiled but charged particle and photon reactions had received less attention. This experimental data can be used to evaluate and enhance theoretical models of neutron, photon, and charged particles induced reactions [10].

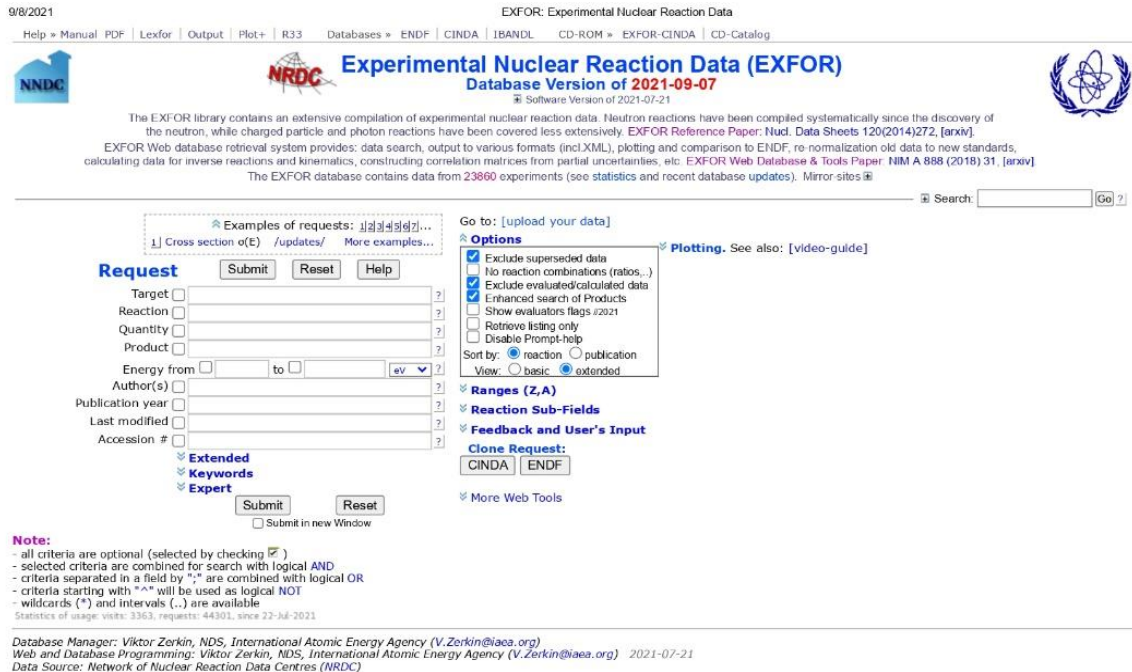


Fig. 1.3 The GUI of the EXFOR database.

## 1.2.2 Evaluated Nuclear Data File (ENDF)

The Evaluated Nuclear Data Library (ENDF) contains reaction data with a focus on the data requirements of fusion and fission research facilities. The GUI of the ENDF database is shown in Fig. 1.4. The result of an evaluation is stored as a set of data files in different Evaluated Nuclear Data File (ENDF) format. The Evaluated Nuclear Data File (ENDF), the Japanese Evaluated Nuclear Data Library (JENDL), the Fusion Evaluation Nuclear Data Library (FENDL), the Chinese Evaluation Neutron Data Library (CENDL), Talys Evaluation Nuclear Data Library (TENDL), and the Joint Evaluated Fission and Fusion File (JEFF) are the most often used evaluated libraries. The National Nuclear Data Center (NNDC) in the United States, the Japan Atomic Energy Agency (JAEA), and the Nuclear Energy Agency

(NEA) of the Organisation for Economic Cooperation and Development (OECD) manage the ENDF, JENDL, and JEFF data respectively. These libraries are the most up-to-date representations of nuclear data observables [11-16].

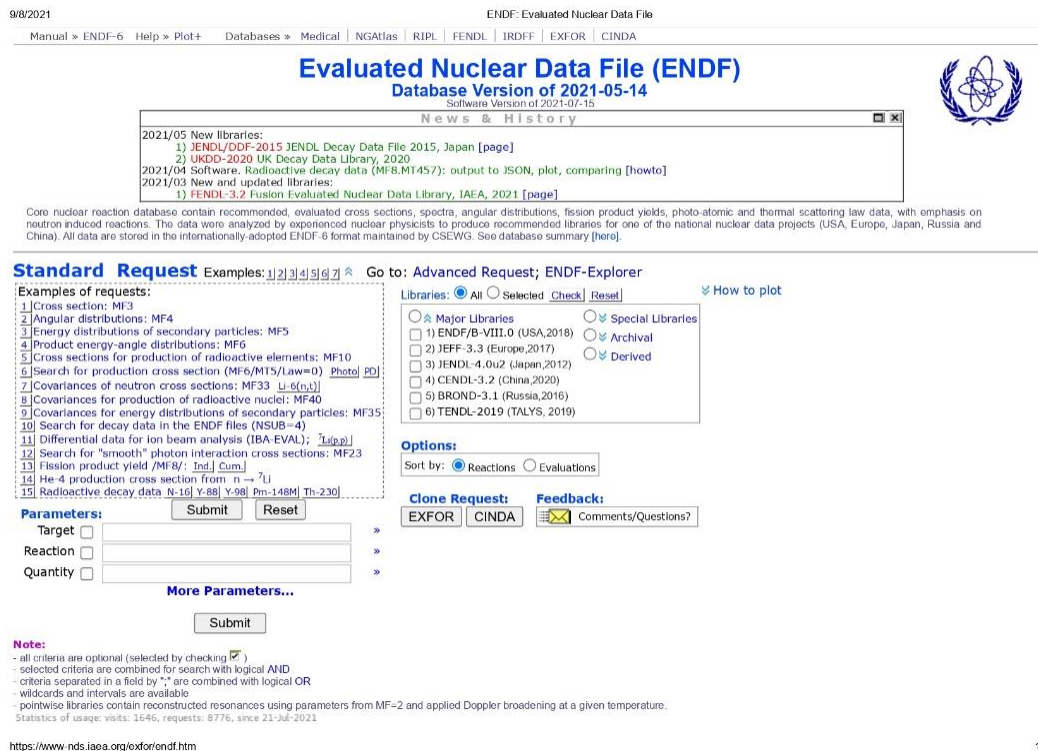


Fig. 1.4 The GUI of the ENDF database.

### 1.2.3 Reference Input Parameter Library (RIPL-3.0)

The Reference Input Parameter Library (RIPL) is a database containing essential input parameters needed in calculations of nuclear reactions and data evaluations. The GUI of the RIPL database is shown in Fig. 1.5. This comprises ENSDF evaluated structural data and reaction model inputs like the masses, discrete levels, neutron resonance, optical model, level densities gamma and fission. This library proposes values or models for reaction calculations based on the reviewed structural information, experimental data, and theory work. This library is a single database that contains most of the nuclear data required to execute the reaction calculation algorithms and ensures that the calculations are accurate and consistent [17].

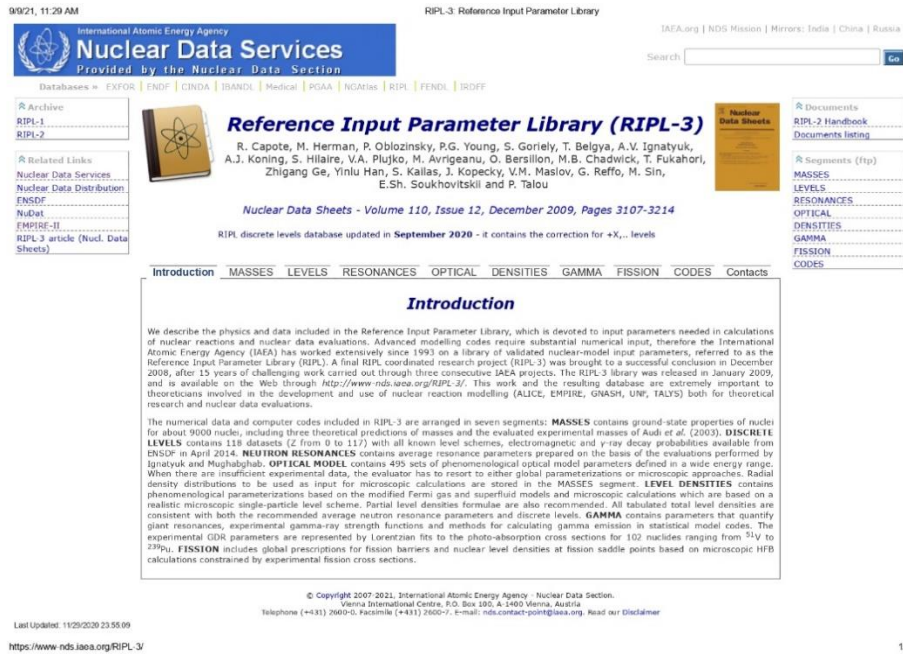


Fig. 1.5 The GUI of the RIPL database.

## 1.2.4 National Nuclear Data Center (NuDat. 3.0)

Now users can interactively search for nuclear structure and decay data using the NuDat web application. At Brookhaven National Laboratory, the National Nuclear Data Center (NNDC) was created NuDat at the website <http://www.nndc.bnl.gov>. The GUI of the NuDat. 3.0 database is shown in Fig. 1.6. It serves as a connection point between web users and several databases that include data on nuclear structure, nuclear decay, and some neutron induced nuclear reactions.

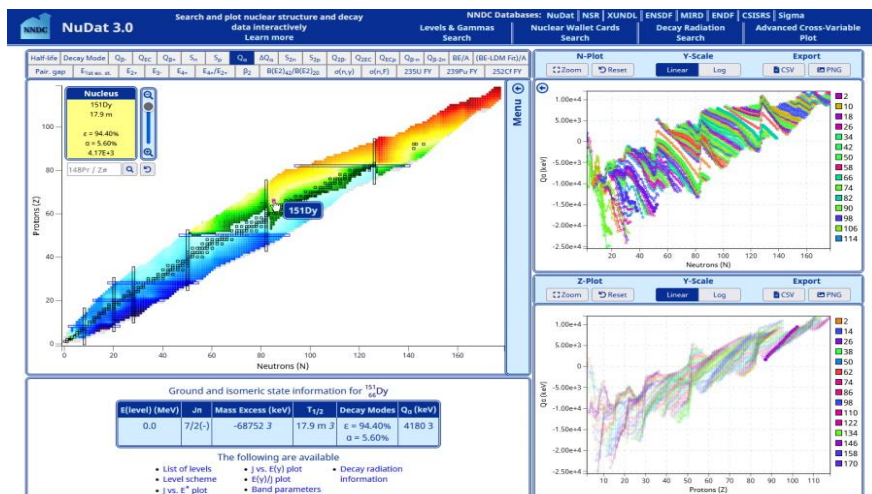


Fig. 1.6 The GUI of the NNDC database.

## 1.3 Literature survey and uncertainties in the nuclear data

The neutron induced reactions cross sections for Se, Cu, Ti, Cr, V, Rh, and Sb elements have been studied in the present thesis. The experimental data are taken from the EXFOR database and evaluated data from the ENDF database. More details for the selected reactions channels are mentioned below:

### 1.3.1 Vanadium and Copper

Several authors studied the  $(n, p)$  reaction cross section of the  $^{65}\text{Cu}$  and  $^{51}\text{V}$  isotope as mentioned in the literature. These experimental cross sections data are reported in the EXFOR database [10] were measured using neutrons from the D-D and D-T reactions, whereas only one datum in the quasi-monoenergetic neutrons was produced based on  $^9\text{Be}(p, n)$  reaction neutrons. The existing experimental and evaluation of the  $^{65}\text{Cu}(n, p)^{65}\text{Ni}$  and  $^{51}\text{V}(n, p)^{51}\text{Ti}$  reactions from threshold to 22 MeV are shown in Fig. 1.7. These available experimental data are agreed very well with each other below 12 MeV but reveal huge discrepancies in cross section above 13 MeV. There are also significant differences in the evaluated  $(n, p)$  reaction cross section of the  $^{65}\text{Cu}$  isotope above the neutron energy of 14 MeV, which were found in many Evaluated Nuclear Data File (ENDF) libraries. Due to the significant spread in the measured cross section values, it is not surprising that the evaluated  $^{65}\text{Cu}(n, p)^{65}\text{Ni}$  reaction cross section varies significantly above the neutron energies of 12 MeV, making it very uncertain extrapolating to higher energies. Similarly, the previously existing literature datasets for  $^{51}\text{V}(n, p)^{51}\text{Ti}$  reaction are presented in Fig. 1.7. The cross sections obtained from the evaluations of JENDL/AD-2017, ENDF/B-VIII.0 and TENDL-2019 libraries are in good agreement with each other from threshold to 14 MeV energies region, whereas at above 14 MeV the cross section of JENDL/AD-2017 libraries shows lower values of cross section compared to the TENDL-2019 and ENDF/B-VIII.0 libraries as shown in Fig. 1.7. The data of A. Fessler shows the lower value of cross section compared to the data of M. Borman *et al.* within 16–19 MeV energies. The significant discrepancies in the measured  $(n, p)$  reaction cross section above 12 MeV were the main reason for the present study at higher neutron energies.

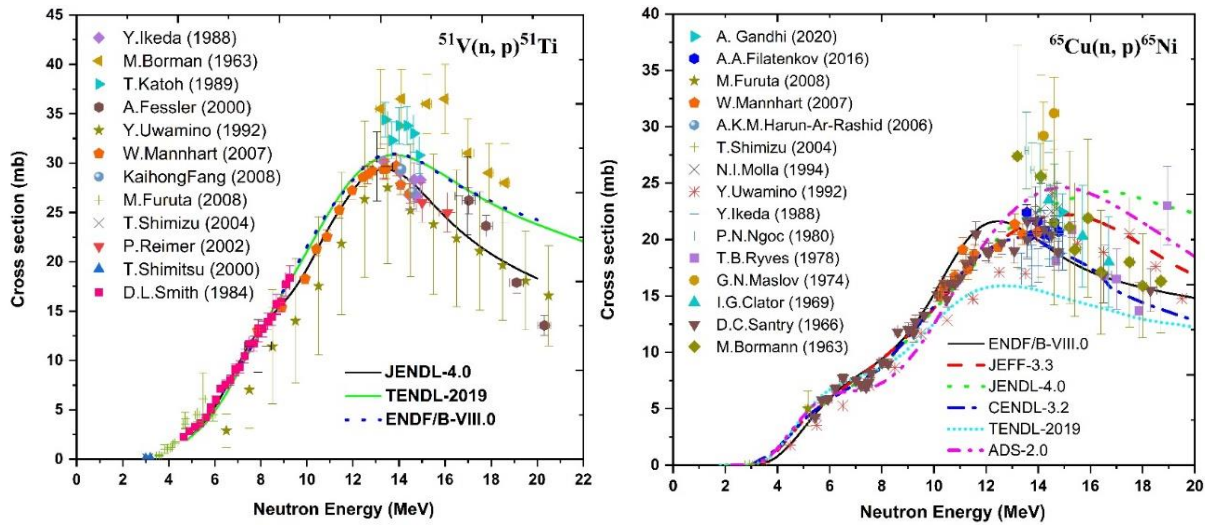


**Fig. 1.7** The comparison of the existing datasets in the literature and evaluated data for the  $^{51}\text{V}(n, p)^{51}\text{Ti}$  and  $^{65}\text{Cu}(n, p)^{65}\text{Ni}$  reactions cross section.

### 1.3.2 Selenium

The previous experimental results are mentioned in Fig. 1.8 along with the evaluated data. It is observed that the experimental data are available only in 13-16 MeV region for the  $^{77}\text{Se}$  and  $^{82}\text{Se}$  isotopes, whereas there is only one measured data below 13 MeV for the  $^{76}\text{Se}$  and  $^{78}\text{Se}$  isotopes. In literature for the  $^{76}\text{Se}(n, p)^{76}\text{As}$  reaction, the large difference between ENDF/B-VIII.0 and JENDL-4.0, TENDL-2019 evaluated data can be seen in 7 to 14 MeV energy range and at higher energy. Similarly, for the  $^{77}\text{Se}(n, p)^{77}\text{As}$  reaction, the TENDL-2019 evaluation is higher in the 7 to 18 MeV energy region are compared to the JENDL-4.0 and ENDF/B-VIII.0. Furthermore, the TENDL-2019 evaluation is very high in between 12 to 22 MeV region compared to the JENDL-4.0 and ENDF/B-VIII.0 for the  $^{78}\text{Se}(n, p)^{78}\text{As}$  reaction, whereas the large difference between JENDL-4.0, TENDL-2019 and ENDF/B-VIII.0 evaluated data are also observed at above 14 MeV energy region for the  $^{80}\text{Se}(n, p)^{80}\text{As}$  reaction. These reported experimental data show significant discrepancies, whereas the evaluated data are also show disagreement with each other at the same energies.

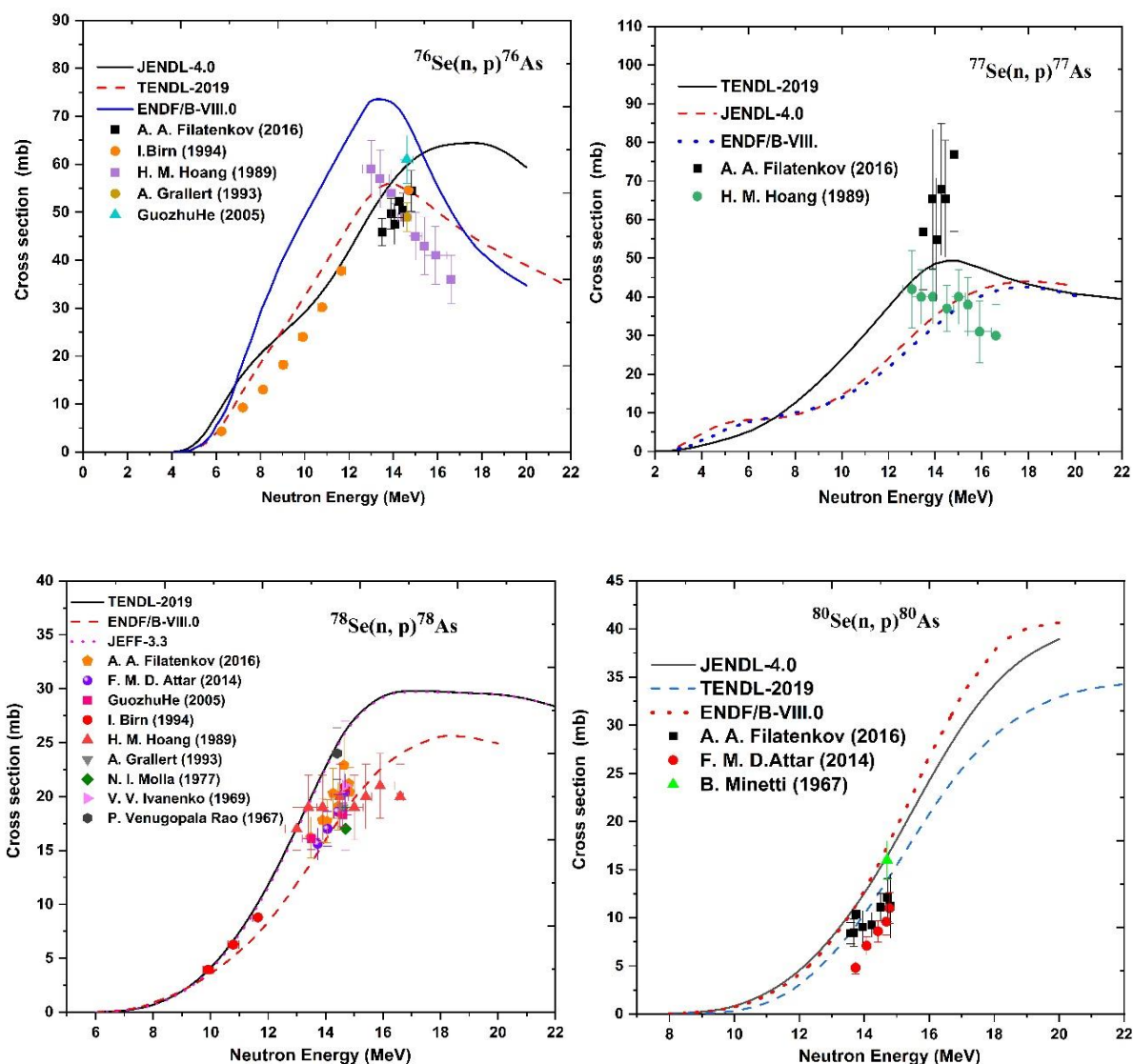


**Fig. 1.8** The comparison of the existing datasets in the literature and evaluated data for the  $\text{Se}(n, p)\text{As}$  reactions cross section of  $^{76,77,78,80}\text{Se}$  isotopes.

### 1.3.3 Antimony and Rhodium

The reported experimental results of the  $^{121}\text{Sb}(n, 2n)^{120}\text{Sb}^m$  and  $^{123}\text{Sb}(n, 2n)^{122}\text{Sb}$  reactions were compared with the latest evaluated data libraries as shown in Fig. 1.9. In literature for the isomeric state cross section of the  $^{121}\text{Sb}(n, 2n)^{120}\text{Sb}^m$  reaction is reported from 13-20 MeV energies. At 14 MeV data of N. L. Das *et al.*, W. D. Lu *et al.*, Y. Kanda *et al.* and A. Reggoug *et al.* agree, whereas other data are very discrepant. However, for the  $^{123}\text{Sb}(n, 2n)^{122}\text{Sb}$  reaction results of W. D. Lu *et al.* and S. K. Ghorai *et al.* agree with the

result of the JENDL/AD-2017 evaluation within experimental uncertainties. Similarly, the results of N. L. Das *et al.* and J. Luo *et al.* agree very well with the JEFF-3.3 evaluation. As can be seen, the measured experimental data of A. A. Filatenkov, J. Frehaut *et al.* and L. R. Vesser *et al.* show good agreement with the evaluated data of the ENDF/B-VIII.0 and JENDL-5.0 libraries within experimental uncertainties.

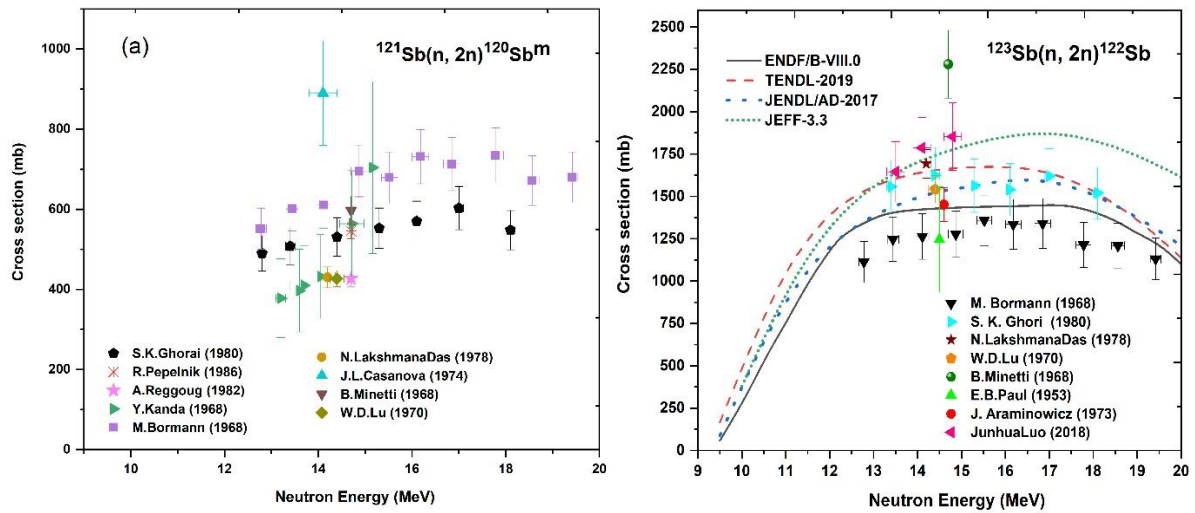


**Fig. 1.9** The comparison of existing literature and evaluated data of the  $^{121}\text{Sb}(n, 2n)^{120}\text{Sb}^m$  and  $^{123}\text{Sb}(n, 2n)^{122}\text{Sb}$  reactions.

The reported measured cross sections of the  $^{103}\text{Rh}(n, 2n)^{102}\text{Rh}$  reaction were compared with the latest evaluated data libraries as shown in Fig. 1.10. As can be seen, the measured experimental data of A. A. Filatenkov, J. Frehaut *et al.* and L. R. Vesser *et al.* show good agreement with the evaluated data of the ENDF/B-VIII.0 and JENDL-5.0 libraries within experimental uncertainties. In contrast, the reported measured data of A. Paulsen *et al.*, D. G. Vallis *et al.* and H. A. Tewes *et al.* show lower values of cross section compared to the latest evaluated data. The available literature data are very discrepant from threshold to 25 MeV.

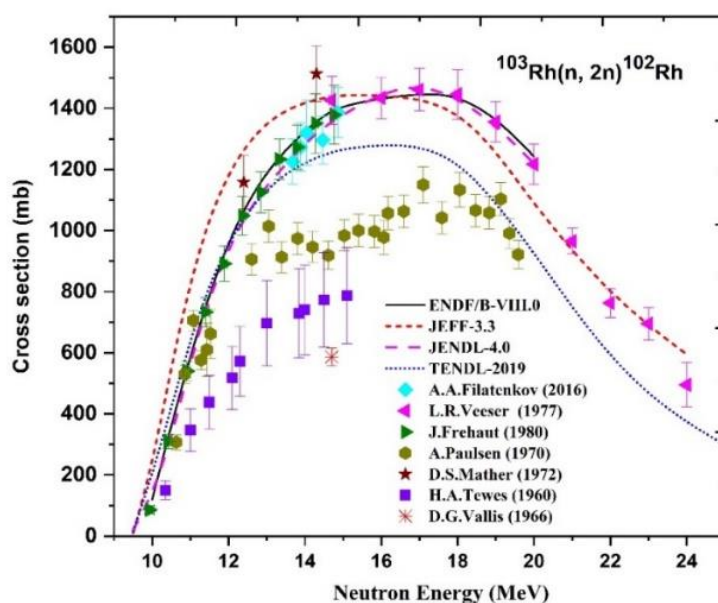


**Fig. 1.10** The comparison of the existing datasets in the literature and evaluated data for the  $^{103}\text{Rh}(n, 2n)^{102}\text{Rh}$  reaction cross section.

### 1.3.4 Chromium and Titanium

The excitation function for the  $^{52}\text{Cr}(n, p)^{52}\text{V}$  reaction, along with the latest evaluated data libraries, is shown in Fig. 1.11. Below 9 MeV neutron energy W. Mannhart *et al.* and D. L. Smith *et al.* reported the measured cross sections. In this region, there is no contribution from the  $^{53}\text{Cr}(n, np)^{52}\text{V}$  and  $^{53}\text{Cr}(n, d)^{52}\text{V}$  reactions since the reaction threshold energies are 11.34 and 9.07 MeV, respectively. Hence measurements carried out using a natural sample of chromium give a pure  $^{52}\text{Cr}(n, p)^{52}\text{V}$  reaction cross section. As shown in Fig. 1.11, the measured cross sections of W. Mannhart *et al.*, A. Fessler *et al.* and D. L. Smith *et al.* agree very well with the FENDL-3.2b and CENDL-3.2 evaluation and are in fair agreement with TENDL-2019, ENDF-B/VIII.0 and JENDL-5.0 libraries. It is worth mentioning that at around 14–15 MeV neutron energy where multiple measured data are available, the data are agree with each other within 10%, whereas the data from S. K. Ghorai *et al.*, I. G. Clator and B. D. Kern *et al.* are either too high or too low and there is no consistent agreement among them. Above 14 MeV incident neutron energy, all the measured cross sections show different values above or below the evaluated cross section data. The measured data by S. K. Ghorai *et al.* around 14 MeV deviate too much from all existing measured cross sections, and the true excitation curve does

not seem to follow the trend of this data set, because measured data below 12 MeV neutron energy are quite accurate and the contribution from the  $^{53}\text{Cr}(n, x)^{52}\text{V}$  reaction is zero or negligibly small.

Similarly, the excitation function of the  $^{48}\text{Ti}(n, p)^{48}\text{Sc}$  reaction, along with the reported measured and evaluated data libraries is shown in Fig. 1.11. A good agreement among literature data has been found within experimental uncertainties except with the few data, probably due to the use of old nuclear decay data and monitor values in those analyses. Many labs measured these reported cross section and there is a large discrepancy in the cross sections in the energy region of 13-16 MeV. Below 13 MeV, the  $^{48}\text{Ti}(n, p)^{48}\text{Sc}$  reaction was studied in various previous measurements and the latest TENDL-2019, FENDL-3.2b, JENDL-5.0 and CENDL-3.2 evaluation reproduces the previous experimental data well. The evaluation follows the measurements up to 13 MeV and is different in values above 13 MeV energies. At energies above 14 MeV, the latest evaluated data JENDL-5.0 is 10 % higher than the evaluated data of the CENDL-3.2 library. It's observed that the high energies data of Y. Uno *et al.* follow the trend of evaluated data of the TENDL-2019 library. However, above 15 MeV the reported data of Lu Hanlin *et al.* H. L. Pai *et al.* M. Bormann *et al.* and F. Gabbard *et al.* show agreement with the evaluated data within experimental uncertainties.

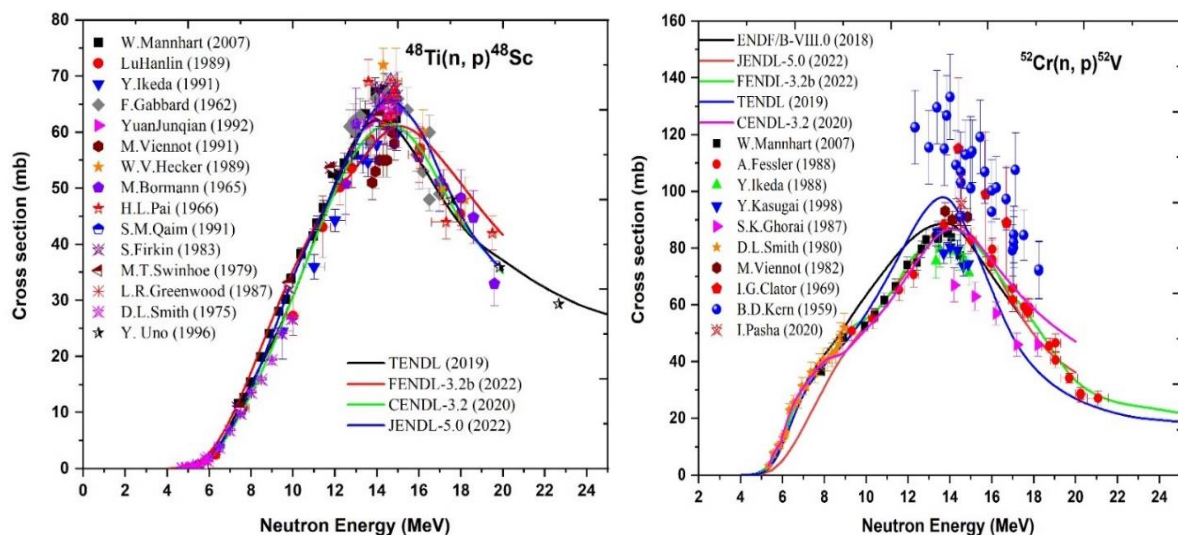


**Fig. 1.11** The comparison of existing datasets in literature and evaluated data for the  $^{48}\text{Ti}(n, p)^{48}\text{Sc}$  and  $^{52}\text{Cr}(n, p)^{52}\text{V}$  reactions cross section.

## 1.4 Motivation and objective

In literature, a significant amount of research has been done to understand the nuclear processes in the low to moderate energy range using  $(n, \gamma)$ ,  $(n, p)$ ,  $(n, 2n)$ ,  $(n, \alpha)$  etc. reactions channels. The neutron induced  $(n, p)$  and  $(n, 2n)$  reactions cross sections for the selected Se, Cu, Ti, Cr, V, Rh, and Sb elements are taken from the experimental EXFOR database and evaluated data from the ENDF database. It is observed that the literature cross section shows large discrepancies in the available experimental and evaluated data at the same incident neutron energies. However, the previous measurement was restricted to energy values around 14 MeV incident neutron energies and there are inconsistent experimental results for the selected elements. More experimental data seems necessary for energies below 13 and above 15 MeV energies. The measured cross section data is scarce for neutron energy greater than 15 MeV. The experimental mapping of the  $(n, 2n)$  and  $(n, p)$  excitation functions is needed for an extended high energy region. In the literature review, the few previous measurements used a coincidence setup of two NaI(Tl) detectors to count the annihilation  $\gamma$ -rays of the positrons from the  $\beta^+$  decay of the reaction product nucleus. The use of the NaI(Tl) detector for  $\gamma$ -ray or  $\beta$ -ray counting has a resolution problem. The recent works use high resolution HPGe  $\gamma$ -ray spectroscopy to measure the activated samples.

The main objective of the present thesis is to study and investigate the neutron induced reaction cross sections on Se, Cu, Ti, Cr, V, Rh, and Sb elements using neutron activation and offline  $\gamma$ -ray spectrometry. In order to extend the excitation function to higher energies, where no data are available, and to resolve discrepancies in the data for the  $(n, 2n)$  and  $(n, p)$  reactions above 14 MeV, the advanced theoretical calculations using the latest codes Talys (ver. 1.9) and EMPIRE (ver. 3.2) [18-19] were performed to test the reliability of the different theoretical models in the present work. To validate the theoretical estimations and improve the parameterization of the statistical model calculations, both codes were tested with different input parameters.

## 1.5 Outline of the thesis

The present Ph.D. thesis work is divided into seven chapters as follows:

➤ **Chapter 1**

Chapter 1 gives a broad overview of nuclear reactions and nuclear data. Neutron-induced reactions are given special attention, and their significance is explained in this chapter. Furthermore, the status of nuclear data and its use in various energy regions were discussed briefly. This chapter also includes an overview of the neutron-induced reaction cross sections and the uncertainties in the measured cross section.

➤ **Chapter 2**

Chapter 2 describes the irradiation experimental setup. The neutron facility and sample details are briefly stated in this chapter. Moreover, the experimental design used for irradiation as well as the HPGe detector setup used for activated measurement is described in this chapter.

➤ **Chapter 3**

Chapter 3 deals with the procedures for data analysis work in which the activation cross section calculation and uncertainties in the measured cross sections are described systematically using the covariance method. In addition, the different systematic formulae for the estimates of the  $(n, p)$  and  $(n, 2n)$  reactions cross sections are included in this chapter.

➤ **Chapter 4**

Chapter 4 illustrates the statistical model calculations based on the level density, optical potential, and pre-equilibrium models. The different nuclear reaction models and two different simulation codes TALYS (ver. 1.9) and EMPIRE (ver. 3.2.3) were used for the theoretical calculations and details about the codes are explained in this chapter.

➤ **Chapter 5**

Chapter 5 discusses the neutron induced  $(n, 2n)$  reaction cross sections for  $^{103}\text{Rh}$ ,  $^{121}\text{Sb}$  and  $^{123}\text{Sb}$  isotopes. The present results are compared with the previous measurements and latest evaluations of the ENDF/B-VIII.0, JEFF-3.3, JENDL-4.0/HE, CENDL-3.2, TENDL-2019 and FENDL-3.2 libraries. We also compare the experimental results with theoretical estimates using TALYS (ver. 1.95) and EMPIRE (ver. 3.2.3) codes from the reaction threshold to the 25 MeV energy region. Furthermore, the  $(n, 2n)$  reactions cross section of the  $^{103}\text{Rh}$ ,  $^{121}\text{Sb}$  and  $^{123}\text{Sb}$  isotopes are estimated within 14-15 MeV neutron energies using different systematic formulae are discussed in details. These estimated cross sections by various systematic formulae are compared with the previous experimental data.

## ➤ **Chapter 6**

Chapter 6 explains the neutron induced ( $n, p$ ) reaction cross sections for  $^{76,77,78,80}\text{Se}$ ,  $^{65}\text{Cu}$ ,  $^{52}\text{Cr}$ ,  $^{51}\text{V}$  and  $^{48}\text{Ti}$  isotopes. The present results are compared with the previous measurements and latest evaluations of the ENDF/B-VIII.0, JEFF-3.3, JENDL-4.0/HE, CENDL-3.2, TENDL-2019 and FENDL-3.2 libraries. The present experimental results also compare with the theoretical estimates using TALYS (ver. 1.95) and EMPIRE (ver. 3.2.3) codes from reaction threshold to the 25 MeV neutron energy region. Furthermore, the ( $n, p$ ) and ( $n, \alpha$ ) reactions cross section of the  $^{76,77,78,80}\text{Se}$ ,  $^{65}\text{Cu}$ ,  $^{52}\text{Cr}$ ,  $^{51}\text{V}$  and  $^{48}\text{Ti}$  isotopes are estimated within 14-15 MeV neutron energies using different systematic formulae and discussed in details. These calculated cross sections by various systematic formulae are compared with the previous experimental data.

## ➤ **Chapter 7**

Chapter 7 summarizes the results and conclusions of the research work described in the present thesis and proposals for future work indicated in this chapter.

## ***Bibliography***

- [1] E. Dupont, M. Bossant, R. Capote, *et al.*, EPJ Web Conf. 239, 15005 (2020).
- [2] E. Georgali, N. Patronis, A. Anastasiadis, *et al.*, Phys. Rev. C 104, 064603 (2021).
- [3] S. Goriely, S. Hilaire, and A. J. Koning, Astron. Astrophys. 487, 767 (2008).
- [4] Gy. Gyurky, Zs. Fulop, F. Kappeler *et al.*, Eur. Phys. J. A (2019) 55: 41.
- [5] J. Ongena, G.V. Oost, Fusion Sci. Technol. 53, 3 (2012).
- [6] Swedish Nuclear Fuel and Waste Management Co, ISSN 1402–3091, SKB Rapport On fusion driven systems (FDS) for transmutation, R-08–126 (2008).
- [7] D. L. Smith, B. A. Loomis, and D. R. Diercks, Journal of Nuclear Materials 135, 125-139 (1985).
- [8] Karolina Kolos, Vladimir Sobes *et al.*, Phys. Rev. Res. 4, 021001 (2022).
- [9] D. D. Sood, M. Herman, O. Schwerer *et al.*, Journal of Radioanalytical and Nuclear Chemistry Vol. 243 No. 1 (2000) 227-233.
- [10] N. Otuka, E. Dupont, V. Semkov, *et al.*, Experimental Nuclear Reaction Data (EXFOR), Nuclear Data Sheets Volume 120, Pages 272-276, June (2014).

- [11] D. A. Brown, M. B. Chadwick, R. Capote, *et al.*, “EDNF/B-VIII.0.” Nuclear Data Sheets 148, 1-142 (2018).
- [12] P. Pereslavtsev, A. Konobeyev, *et al.*, JEFF-3.3, Evaluation nuclear data library of the OECD Nuclear Energy Agency, JEF/DOC, p. 1864 (2017).
- [13] S. Kunieda *et al.*, "Overview of JENDL-4.0/HE and benchmark calculation" JAEA-Conf 2016-004, pp. 41-46 (2016).
- [14] K. XU, H. X. AN, C. H. CAI, H. C. WU, CENDL-3.2 Chinese evaluation neutron data library, issued in (2020).
- [15] A. J. Koning, D. Rochman, J.-Ch. Sublet, *et al.*, “TENDL-2019” Nuclear data sheets Vol. 155, 1-55 (2019).
- [16] R. A. Forrest, R. Capote, N. Otsuka, *et al.* FENDL-3.2 Fusion Evaluation Nuclear Data Library, IAEA, INDC (NDS)-0628 (2021).
- [17] R. Capote, M. Herman, P. Oblozinsky *et al.*, “RIPL – Reference Input Parameter Library for Calculation of Nuclear Reactions and Nuclear Data Evaluations” Nuclear Data Sheets 110 (2009) 3107–3214.
- [18] A. J. Koning, *et al.*, TALYS (ver. 1.96), A Nuclear reaction program, user manual, NRG-1755 ZG Petten, The Netherlands (2018).
- [19] M. Herman, R. Capote, M. Sin *et al.* “EMPIRE-3.2.2 Statistical Model Code for Nuclear Reaction Calculations and nuclear data evaluation” Nucl. Data Sheets 108, 2655 (2007).